Bioorganic & Medicinal Chemistry 17 (2009) 7275–7280

Contents lists available at ScienceDirect

Bioorganic & Medicinal Chemistry

journal homepage: www.elsevier.com/locate/bmc

Synthesis and hybridization of 2′-*O*-methyl-RNAs incorporating 2′-*O*-carbamoyluridine and unique participation of the carbamoyl group in U–G base pair

Kohji Seio *, Ryuya Tawarada, Takeshi Sasami, Masashi Serizawa, Misako Ise, Akihiro Ohkubo, Mitsuo Sekine *

Department of Life Science, Tokyo Institute of Technology, 4259 Nagatsuta, Yokohama 226-8501, Japan

ARTICLE INFO

Article history:
Received 30 June 2009
Revised 20 August 2009
Accepted 21 August 2009
Available online 2 September 2009

Keywords:
2′-*O*-Modified-RNA
Mismatched base pair

ABSTRACT

2′-*O*-Carbamoyluridine (U_{cm}) was synthesized and incorporated into DNAs and 2′-*O*-Me-RNAs. The oligonucleotides incorporating U_{cm} formed less stable duplexes with their complementary and U_{cm}–U, U_{cm}–C single-base mismatched DNAs and RNAs in comparison with those without the carbamoyl group. On the contrary, the T_m analyses revealed that the duplexes with a mismatched U_{cm}–G base pair showed almost the same thermostability as the corresponding unmodified duplexes. Molecular dynamics (MD) simulations of the U_{cm}-modified 2′-*O*-Me-RNA/RNA duplexes with U_{cm}–G mismatched base pair suggested that the carbamoyl group could participate in the U_{cm}–G base pair by an additional intermolecular hydrogen bond between the carbamoyl oxygen and the H2 of the guanine base.

1. Introduction

2′-*O*-Modified RNA molecules have been extensively used for gene regulation such as antisense, antigene, and RNA interference (RNAi) strategies[1–4] and microRNA analysis.[5] Modification of RNAs could improve their stability toward hydrolysis by nucleases and enhance their hybridization affinity for the target RNAs.[6] Most of the 2′-*O*-substituents reported to date were comprised of ether-type skeletons in which the 2′-oxygen attaches to sp^3-type carbon atoms of various functional groups such as 2′-*O*-methyl,[7] 2′-*O*-methoxyethyl,[8–15] 2′-*O*-propargyl,[16] 2′-*O*-aminopropyl,[17] 2′-*O*-dimethylaminopropyl,[18] 2′-*O*-[2-(methylamino)-2-oxoethyl],[19,20] and 2′-*O*-(2-cyanoethyl).[21]

In this paper, we report the synthesis and hybridization properties of 2′-*O*-methyl-RNA incorporating 2′-*O*-carbamoyluridine. We have been interested in this type of modification in consideration of its potential utility because of the following reasons: (a) since the polarized carbonyl part of the carbamoyl group is more hydrophilic than the sp^3-type alkyl carbon of 2′-*O*-ethereal substituents, such a modification might enhance a hydration network around the minor groove.[22–24] (b) Since the carbamoyl group contains a carbonyl oxygen and two amino protons as hydrogen bond donor and acceptor sites, respectively, it can form unique hydrogen bonds both intramolecularly and intermolecularly.[25–27] (c) Introduction of the carbamoyl group into the 2′-hydroxyl group could be performed by simple reaction of an appropriately protected nucleoside derivative with phenyl chloroformate followed by substitution with ammonia. In contrast, introduction of ether-type substituents usually required proton abstraction from the 2′-hydroxyl group by strong bases, which cause damage on the protecting groups in the base and sugar moieties. (d) While most of the acyl-type substituents at the 2′-*O*-position are unstable under basic conditions, and they easily migrate to the neighboring 3′-hydroxyl group even under the neutral conditions upon removal of the neighboring 3′-protecting group, the carbamoyl group is exceptionally stable under the same conditions.

In this paper, we report the details of the hybridization properties of DNA and 2′-*O*-methyl-RNA (2′-*O*-Me-RNA) oligomers incorporating U_{cm}. Molecular dynamics (MD) simulations of modified 2′-*O*-Me-RNA/RNA duplexes indicated a unique hydrogen bond between the carbamoyl oxygen of U_{cm} and the H2 of G in the U_{cm}–G mismatched base pair.

2. Results and discussion

2.1. Synthesis of 2′-*O*-carbamoyluridine and its derivatives

Synthesis of 2′-*O*-carbamoyluridine **4** and its phosphoramidite derivative **5** was performed as shown in Scheme 1. 3′,5′-*O*-(1,1,-3,3-Tetraisopropyldisiloxane-1,3-diyl)uridine[28] was converted to the 2′-*O*-phenoxycarbonyl derivative **1** with a 79% yield by treatment with 1.2 equiv of phenyl chloroformate. The carbonate **1**

* Corresponding authors. Tel.: +81 45 924 5706; fax: +81 45 924 5772.
E-mail addresses: kseio@bio.titech.ac.jp (K. Seio), msekine@bio.titech.ac.jp (M. Sekine).

0968-0896/$ - see front matter © 2009 Elsevier Ltd. All rights reserved.
doi:10.1016/j.bmc.2009.08.053

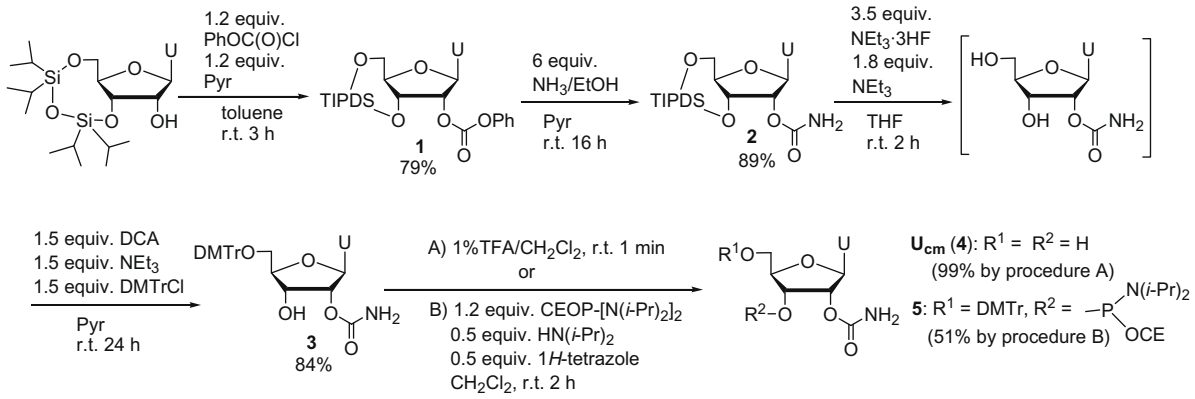

Scheme 1. Synthesis of 2′-*O*-carbamoyluridine derivatives.

was ammonolyzed to give the carbamate **2** with an 89% yield. Then, the silyl-protecting group was removed using 3.5 equiv of triethylamine–trihydrofluoride,[29] and the resulting 5′-hydroxyl group was protected with a DMTr group without separation of the triethylammonium salt to give **3**. In this reaction, addition of $Cl_2CHCOOH$ (DCA) and triethylamine[30] to the deprotection mixture proved to be effective. Finally, compound **3** was converted to the nucleoside **4** and the phosphoramidite **5** by standard procedures.

2.2. Sugar conformation of 2′-*O*-carbamoyluridine

The sugar conformation property of 2′-*O*-carbamoyluridine (**4**: U_{cm}) was analyzed using the ^1H–^1H coupling constants between the sugar protons. In general, the ribose conformation of nucleosides could be estimated by the equilibrium between the N-type and S-type conformers, and the population of the N-type conformation (%N) could be calculated by dividing $J_{3'4'}$ by $J_{1'2'} + J_{2'3'}$.[31] U_{cm} values are shown in Table 1 along with the coupling constants of uridine (U) and 2′-*O*-methyluridine (U_{OMe}). It was revealed that the %N values of the ribose moieties of U and U_{cm} were 56% and 57%, respectively, and almost identical. Moreover, the %N value of U_{cm} differed from that of U_{OMe} by only 3%.

These results indicated that conformation property of U_{cm} was essentially identical to that of U and U_{OMe}, and oligonucleotides incorporating U_{cm} were expected to preferably form A-type duplexes upon hybridization with the complementary DNA and RNA oligomers.

2.3. Hybridization properties of DNAs and 2′-*O*-Me-RNAs incorporating U_{cm}

Next, we examined the hybridization properties of DNA and 2′-*O*-Me-RNA incorporating U_{cm}. Previously, studies on the synthesis, hybridization properties, and structure of DNAs incorporating a 2′-*O*-(*N*-methylcarbamoyl)ribothymidine (2′-*O*-NMC-T) were reported,[20,32] and it was concluded that incorporation of 2′-*O*-NMC-T into DNA reduced the affinity of the modified DNA for the complementary RNA due to the dipole–dipole interaction between the carbonyl oxygen at position 2 of uracil and the carbamoyl group. However, detailed hybridization properties such as the base discrimination of the 2′-*O*-NMC-T were not reported. In this study, we carried out more detailed experiments for the hybridization of DNA duplexes incorporating U_{cm} as well as the base recognition properties of U_{cm} in these duplexes. We also studied the stability of 2′-*O*-Me-RNA/RNA duplexes incorporating U_{cm}. The nucleotide sequences used in these experiments are shown in Figure 1 and the T_m results are shown in Tables 2 and 3.

As shown in Table 2, the DNA–DNA duplexes consisted of **DNA2** incorporating U_{cm} showed lower T_m than those consisting of the unmodified DNA (**DNA1**) irrespective of the base pairing partner at position X. This observation agreed with the hybridization properties of oligodeoxynucleotides containing 2′-*O*-NMC-T, which showed marked decrease in the affinity of the modified DNA due to the dipole–dipole repulsion between the carbonyl groups. In the case of **DNA2**, the T_m decrease (ΔT_m) was the largest (−11 °C) when U_{cm} and A formed a Watson–Crick base pair, as shown in the row of **DNAa**. In contrast, the ΔT_m values of the duplexes of **DNA2** with the target DNAs (**DNAb**, **DNAc**, and **DNAd**) containing a mismatched base were much smaller (by −2 to −6 °C) than that of the duplex with **DNAa**. Consequently, the base recognition accuracy of **DNA2** containing U_{cm} was poorer than that of the unmodified **DNA1**. Interestingly, among the mismatched base pairs, the U_{cm}–G pair showed the smallest destabilization.

Next, we examined the hybridization properties of 2′-*O*-Me-RNA (**Me-RNA2**) incorporating U_{cm}. As shown in Table 3, in the case of **DNAa–d** duplexes, the T_m values of the duplexes of **Me-RNA2**/**DNAa** (X = A), **DNAb** (X = T), and **DNAd** (X = C) were decreased by 8, 10, and 5 °C, respectively, compared with that of the unmodified RNA (**Me-RNA1**). Interestingly, the T_m drop was much smaller (ΔT_m = −2 °C) for the U_{cm}–G mismatched duplex (**Me-RNA2**/**DNAc**). We also studied the thermostability of

Table 1
Ribose puckering (%N) of uridine derivatives

	$J_{1'2'}$	$J_{3'4'}$	$J_{1'2'} + J_{2'3'}$	%N
U	4.4	5.5	9.9	56
U_{OMe}[a]	3.9	5.8	9.7	60
U_{cm}	4.4	5.9	10.3	57

[a] Data from Ref. 21.

DNA1: 5′-d(GTACC**T**TTCCGG)-3′
DNA2: 5′-d(GTACC)[**U_{cm}**]d(TTCCGG)-3′
DNAa-d: 5′-d(CCGGAA**X**GGTAC)-3′
a: X = A; **b**: X = T; **c**: X = G; **d**: X = C

Me-RNA1: 5′-GUACC**U**UUCCGG-3′
Me-RNA2: 5′-GUACC[**U_{cm}**]UUCCGG-3′
RNAa-d: 5′-r(CCGGAA**X**GGUAC)-3′
a: X = A; **b**: X = U; **c**: X = G; **d**: X = C

Figure 1. Nucleotide sequences incorporating U_{cm}. The 2′-*O*-Me-ribonucleotide residues are underlined.

Table 2
T_m (°C) and ΔT_m (°C) of the duplexes of unmodified **DNA1** or U_{cm}-modified **DNA2** and counter strands **DNAa–DNAd**

	DNA1	DNA2	ΔT_m
DNAa X = A	49	38	−11
DNAb X = T	38	32	−6
DNAc Y = G	34	32	−2
DNAd X = C	24	18	−6

ΔT_m = T_m of **DNA2** − T_m of **DNA1**.

Table 3
T_m (°C) and ΔT_m (°C) of the duplexes of unmodified **Me-RNA1** or U_{cm}-modified **Me-RNA2** and the counter strands **DNAa–DNAd** and **RNAa–RNAd**

	Me-RNA1	Me-RNA2	ΔT_m
DNAa X = A	39	31	−8
DNAb X = T	31	21	−10
DNAc X = G	21	19	−2
DNAd X = C	21	16	−5
RNAa X = A	70	65	−5
RNAb X = U	58	54	−4
RNA-c X = G	63	63	0
RNA-d X = C	57	52	−5

Me-RNA2/RNA duplexes. In this case, incorporation of U_{cm} decreased the T_m by 5, 5, and 4 °C when X was A, C, and U, respectively. However, the T_m of **Me-RNA2**/**RNA-c** with a U_{cm}–G mismatch was identical to that of **Me-RNA1**/**RNA-c** with an unmodified U–G mismatch.

Considering the observations shown in Tables 2 and 3, the base pairing property of U_{cm} could be summarized as follows. The incorporation of U_{cm} mostly destabilized DNA/DNA, 2′-*O*-methyl-RNA/DNA, and 2′-*O*-methyl-RNA/RNA duplexes probably due to dipole–dipole repulsion[20] between the carbonyl oxygen at position 2 of the uracil and the carbamoyl group, as suggested in the case of 2′-*O*-NMC-T. Second, although the U_{cm} residue destabilized the duplexes in most cases, the T_m decrease was the smallest in the case of the U_{cm}–G pair in the DNA/DNA and 2′-*O*-Me-RNA/DNA duplexes. In particular, in the case of the 2′-*O*-Me-RNA/RNA duplexes, the duplexes with a U_{cm}–G pair were as stable as those with a U–G pair. These results could be explained by assuming some specific stabilization mechanism of the U_{cm}–G pair by the carbamoyl group. Therefore, we next studied the structure of the duplexes with the U_{cm}–G pair in more detail using their CD spectra and MD simulations.

2.4. CD spectra of duplexes with U_{cm}

The structures of the fully matched modified duplexes, **DNA2**/**DNAa**, **Me-RNA2**/**DNAa**, and **Me-RNA2**/**RNAa**, were studied by measuring their CD spectra, which were then compared with those of the duplexes, **DNA1**/**DNAa**, **Me-RNA1**/**DNAa**, and **Me-RNA1**/**RNAa**, without the carbamoyl modification (Fig. 2A). We also measured the CD spectra of the duplexes, **DNA2**/**DNAc**, **Me-RNA2**/**DNAc**, and **Me-RNA2**/**RNAc**, with a U_{cm}–G mismatch. These CD spectra were also compared with those of **DNA1**/**DNAc**, **Me-RNA1**/**DNAc**, and **Me-RNA1**/**RNAc** without carbamoyl modification (Fig. 2B).

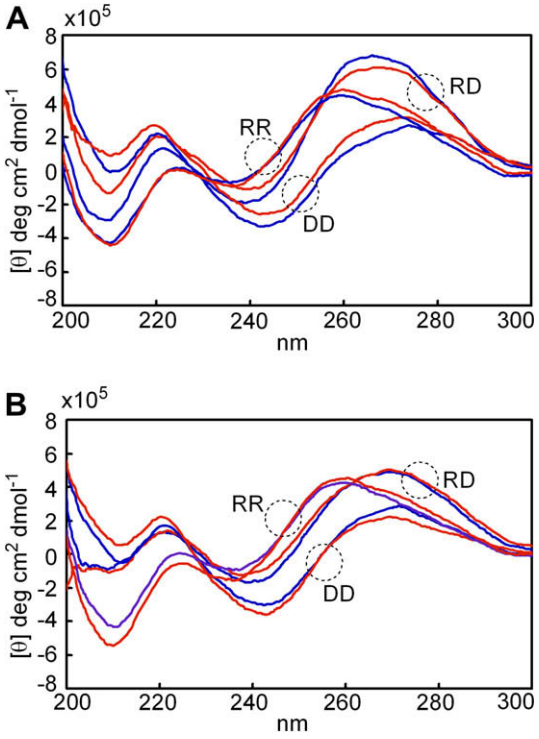

Figure 2. CD spectra of the fully matched (panel A) and U–G mismatched (panel B) duplexes. RD, RR, and DD indicate the category of the duplex types, 2′-*O*-Me-RNA/DNA, 2′-*O*-Me-RNA/RNA, and DNA/DNA duplexes, respectively. The red lines in each category refer to carbamoyl-modified duplexes and the blue lines refer to unmodified duplexes. (panel A) DD-blue: **DNA1**/**DNAa**, DD-red: **DNA2**/**DNAa**; RD-blue: **Me-RNA1**/**DNAa**, RD-red: **Me-RNA2**/**DNAa**; RR-blue: **Me-RNA1**/**RNAa**, RR-red: **Me-RNA2**/**RNAa**. (panel B) DD-blue: **DNA1**/**DNAc**, DD-red: **DNA2**/**DNAc**; RD-blue: **Me-RNA1**/**DNAc**, RD-red: **Me-RNA2**/**DNAc**; RR-blue: **Me-RNA1**/**RNAc**, RR-red: **Me-RNA2**/**RNAc**.

As shown in Fig. 2A, the fully matched DNA/DNA-type (DD) duplexes, such as **DNA1**/**DNA-a** (blue) and **DNA2**/**DNA-a** (red), showed almost identical CD spectra that corresponded to the B-form irrespective of the presence of the carbamoyl group. Such conformational similarities were also observed between **Me-RNA1**/**DNAa** and **Me-RNA2**/**DNAa** in the category of the 2′-*O*-Me-RNA/DNA-type (RD) duplexes, and between **Me-RNA1**/**RNAa** and **Me-RNA2**/**RNAa** in the 2′-*O*-Me-RNA/RNA-type duplexes. As indicated by the shape of the CD spectra,[33] the structures of the DD-, RR-, and RD-type duplexes are considered to exist in B-form, A-form, and one between the A-form and B-form duplexes, respectively, independent of the presence of the carbamoyl group.

Similar conformation properties independent of the carbamoyl modification were also observed in the case of the duplexes containing a G–U mismatch base pair (Fig. 2B). These results suggested that the incorporation of a single carbamoyl group did not affect the structure of these duplexes.

2.5. MD simulation of 2′-*O*-Me-RNA with U_{cm}–G mismatch

MD simulations of the 2′-*O*-Me-RNA-/RNA duplexes incorporating U_{cm} were performed using the AMBER94 force field.[34] The atomic charges for U_{cm} was derived from the ab initio calculations at the HF/6-31G* level. This level of theory was the same as that used in derivatization of the atomic charges of the original AMBER94 parameters. The calculation was performed for **Me-RNA2**/**RNA-b** duplex incorporating U_{cm}–G base pair.

The average structure of the U_{cm}–G pair from the last 200 ps trajectories are shown in Figure 3A. The torsion angle of C3′–C2′–O2′–C(O)NH_2 was in the *anti-periplanar* conformation and the C2′–O2′–C–NH_2 torsion was in the *trans*-conformation. This conformation around the carbamoyl group was identical to those found in the X-ray structure of the (2′-*O*-NMC-T)-A pair in a DNA/RNA duplex.[20]

Interestingly, in this U_{cm}–G pair, in addition to the usual wobble-type base pair between the uracil and the guanine moiety stabilized by the hydrogen bonds between NH3 of uracil and O6 of guanine, and O2 of uracil and NH1 of guanine, the carbonyl oxygen of the carbamoyl group formed an additional third hydrogen bond with NH2 of guanine. This additional hydrogen bond might partly compensate the duplex destabilization effect of the carbamoyl group and contribute to the stability of this U_{cm}–G base pair, as shown in Tables 2 and 3. In several X-ray crystallographic structures of RNA duplexes incorporating G–U mismatches,[35–37] a water molecule bridges the N2 atom of guanine and the O2 atom of uracil. An example of the G–U mismatch pair mediated by a water molecule was reported in Ref. 36 and is shown in Figure 3B. Therefore, the carbamoyl group of U_{cm}–G could be considered to mimic the hydrogen bonding of such a water molecule in the usual U–G mismatch base pair. The geometries of the hydrogen bonds between the carbamoyl group and the nucleobases were not exactly the same as but similar to those of the water molecule as shown in Figure 3. For example, the interatomic distance between the uracil O2 atom and the carbamoyl oxygen was 2.9 Å and that between the oxygen of water was 3.1 Å, as shown in Figure 3A and B, respectively. The same analyses between the N2 atom of guanine and the carbamoyl oxygen (2.8 Å) and the oxygen of water (3.1 Å) also suggested a similar but not identical geometry.

3. Conclusions

We studied the synthesis and properties of U_{cm} and oligonucleotides incorporating U_{cm}. The carbamoyl group did not significantly affect the sugar conformation compared with uridine and 2′-*O*-methyluridine. The introduction of U_{cm} into the duplexes decreased the duplex stability, as suggested previously. The MD simulation revealed some interesting participations of the carbamoyl group in the U_{cm}–G base pair, which could partly explain the stability of the U_{cm}–G base pair suggested in the T_m analysis.

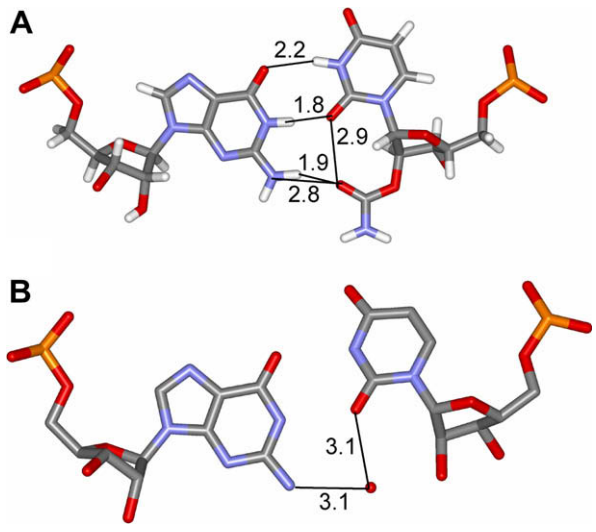

Figure 3. Average structures of the (A) U_{cm}–G base pair. Panel (B) shows the G(13)–U(4) pair mediated by a water molecule found in a crystal.[36] Numbers indicate the distances between the atoms in Å.

Because the introduction of the carbamoyl group into the duplexes reduced the stability of sequence-matched duplexes in all of the DNA/DNA, the 2′-*O*-Me-RNA/DNA, and the 2′-*O*-Me-RNA/RNA cases, the oligonucleotides fully modified with 2′-*O*-carbamoyl groups did not exhibit strong hybridization affinity and hence do not seem applicable. However, we found an interesting ability of the 2′-*O*-carbamoyl group to directly interact with the opposite guanine base to stabilize the U_{cm}–G base pair. These results indicate a new possibility that appropriately designed 2′-*O*-substituents in artificial RNAs can participate in the base pairing with the opposite strands and modulate the base pair stability and selectivity. To the best of our knowledge, such a possibility has not been proposed yet. Therefore, the carbamoyl modification might be useful for nucleotide units that are to be incorporated into appropriate positions of functional nucleic acids, and to modulate their structures and functions with its unique interactions.

Studies on the other 2′-*O*-carbamoyl nucleosides and the duplex stabilization mechanism of the carbamoyl group are currently underway, in addition to the design of new functional groups for the 2′-*O*-position on the basis of the unique results of the present study.

4. Experimental procedures

4.1. General procedures

The dry solvents were purchased and stored over molecular sieves 4 A. ^{1}H, ^{13}C and ^{31}P NMR spectra were obtained at 500, 126 and 203 MHz, respectively. The chemical shifts were measured from tetramethylsilane (0.0 ppm) or DMSO-d_6 (2.49 ppm) for ^{1}H NMR, $CDCl_3$ (77.0 ppm), DMSO-d_6 (39.7 ppm) for ^{13}C NMR and 85% phosphoric acid (0.0 ppm) for ^{31}P NMR. MALDI-TOF and ESI-TOF mass spectra were obtained in the positive ion mode.

4.2. Synthesis of phosphoramidite unit

4.2.1. 2′-*O*-Phenoxycarbonyl-3′,5′-*O*-(1,1,3,3-tetraisopropyldisiloxane-1,3-diyl)uridine 1

3′,5′-*O*-(1,1,3,3-Tetraisopropyldisiloxane-1,3-diyl)uridine (6.1 g, 13 mmol) was dissolved in anhydrous toluene (126 mL) followed by addition of pyridine (1.2 mL, 13 mmol). Next, phenyl chloroformate (1.9 mL. 15 mmol) was added dropwise, and the resulting mixture was stirred for 3 h. The reaction was quenched by addition of water (10 mL), and the solution was diluted with ethyl acetate (200 mL). The organic layer was washed thrice with brine (200 mL × 3), dried over Na_2SO_4, filtered, and evaporated to dryness. The residue was chromatographed on a neutralized silica gel column (180 g) with chloroform–hexane (6:4–4:6, v/v) to give **1** (6.1 g, 79%). ^{1}H NMR ($CDCl_3$) δ 0.97–1.12 (28H, m), 4.03 (1H, dd, J = 2.6 Hz, 11.0 Hz), 4.11 (1H, dd, J = 1.3 Hz, 8.1 Hz), 4.26 (1H, d, J = 3.4 Hz), 4.47 (1H, dd, J = 4.4 Hz, 4.9 Hz), 5.31 (1H, d, J = 4.6 Hz), 5.71 (1H, d, J = 8.0 Hz), 5.93 (1H, s), 7.17 (2H, m), 7.26 (1H, m), 7.38 (2H, m), 7.73 (1H, d, J = 8.0 Hz), 8.28 (1H, s); ^{13}C NMR ($CDCl_3$) δ 13.1, 17.4, 59.6, 68.1, 79.7, 82.2, 88.6, 102.5, 121.1, 126.5, 129.8, 139.5, 149.7, 151.3, 152.4, 162.8. MS *m/z* calculated for $C_{28}H_{43}N_2O_9Si_2^+$ $[M+H]^+$: 607.2502, found: 607.2596.

4.2.2. 2′-*O*-Carbamoyl-3′,5′-*O*-(1,1,3,3-tetraisopropyldisiloxane-1,3-diyl)uridine 2

To the solution of **1** (1.8 g, 3.0 mmol) in anhydrous pyridine (30 mL) was added 2 M NH_3/EtOH (8.9 mL, 17.8 mmol), and the resulting solution was stirred for 16 h. The solution was diluted with ethyl acetate (100 mL) and washed thrice with brine (100 mL × 3), dried over Na_2SO_4, filtered, and evaporated under reduced pressure. The residue was chromatographed on a NH-silica

gel column (50 g) with chloroform–methanol (100:0–100:2, v/v) to give **2** (1.4 g, 89%). ^{1}H NMR ($CDCl_3$) δ 0.93–1.11 (28H, m), 4.00 (2H, m), 4.20 (1H, d, J = 3.5 Hz), 4.39 (1H, dd, J = 3.9 Hz, 5.2 Hz), 4.90 (2H, s), 5.27 (1H, d, J = 5.1 Hz), 5.69 (1H, dd, J = 8.3 Hz), 5.83 (1H, s), 7.64 (1H, d, J = 8.3 Hz), 8.76 (1H, s); ^{13}C NMR ($CDCl_3$) δ 13.2, 17.3, 60.0, 68.1, 76.3, 82.4, 89.0, 102.5, 139.7, 149.9, 155.2, 163.1. MS *m/z* calculated for $C_{22}H_{40}N_3O_8Si_2^+$ $[M+H]^+$: 530.2348, found: 530.2370.

4.2.3. 2′-*O*-Carbamoyl-5′-*O*-(4,4′-dimethoxytrityl)uridine 3

Compound **2** (6.0 g, 11 mmol) was dissolved in anhydrous THF (57 mL). To this solution were added triethylamine (2.7 mL, 20 mmol) and triethylamine trihydrofluoride (6.3 mL, 38 mmol). The resulting solution was stirred for 2 h. The solvents were removed under reduced pressure, and the residual triethylamine and THF were removed by co-evaporation once with toluene and thrice with pyridine, and the residue was finally dissolved in anhydrous pyridine (17 mL). To this solution were added 4,4′-dimethoxytrityl chloride (5.7 g, 17 mmol), triethylamine (2.4 mL, 17 mmol), and dichloroacetic acid (1.4 mL, 17 mmol). After the resulting mixture was stirred for 23 h, the reaction was quenched by addition of methanol (5 mL). The solution was diluted with ethyl acetate (200 mL), washed thrice with brine (200 mL × 3), dried over Na_2SO_4, filtered, and concentrated under reduced pressure. The residual pyridine was removed by co-evaporation with toluene, and the residue was chromatographed on a silica gel column with chloroform–methanol (100:0–100:2, v/v) containing 0.5% triethylamine to give **3** (5.5 g, 84%). ^{1}H NMR ($CDCl_3$) δ 3.44 (2H, m), 3.73 (6H, s), 3.96 (1H, m), 4.16 (1H, d, J = 3.9 Hz), 4.57 (1H, d, J = 4.2 Hz), 5.26 (1H, m), 5.34 (1H, d, J = 8.1 Hz), 5.65 (2H, s), 6.14 (1H, d, J = 5.1 Hz), 6.80 (4H, m) 7.15–7.37 (9H, m), 7.76 (1H, d, J = 8.1 Hz), 9.71 (1H, s); ^{13}C NMR ($CDCl_3$) δ 55.5, 62.8, 70.4, 84.1, 86.8, 87.4, 103.1, 113.6, 127.4, 128.3, 128.4, 130.4, 135.3, 135.5, 140.3, 144.4, 151.2, 156.5, 158.9, 163.6. MS *m/z* calculated for $C_{31}H_{31}N_3NaO_9^+$ $[M+Na]^+$: 612.1925, found: 612.2367.

4.2.4. 2′-*O*-Carbamoyluridine 4

Compound **3** (200 mg, 0.34 mmol) was dissolved in 1% trifluoroacetic acid/CH_2Cl_2 (13 mL). After 1 min, the solution was poured into a suspension of dimethylamino-polystyrene (1 g) in methanol (20 mL). The solids were removed by filtration, and the filtrate was diluted with chloroform (50 mL). The product was extracted with water (50 mL), and the aqueous solution was lyophilized to give **4** (96 mg, 99%). ^{1}H NMR (D_2O) δ 3.84 (1H, dd, J = 4.6 Hz, 10.0 Hz), 3.95 (1H, dd, J = 2.7 Hz, 10.0 Hz), 4.10–4.14 (1H, m), 4.35–4.45 (1H, dd, J = 5.9 Hz, 5.6 Hz), 5.21 (1H, dd, J = 4.4 Hz, 5.6 Hz), 5.92 (1H, d, J = 8.1 Hz), 6.03 (1H, d, J = 4.4 Hz), 7.85 (1H, d, J = 8.1 Hz); ^{13}C NMR (D_2O) δ 60.8, 68.8, 75.6, 84.4, 88.6, 102.7, 142.5, 151.7, 157.8, 166.4. MS *m/z* calculated for $C_{10}H_{14}N_3O_7^+$ $[M+H]^+$: 288.0826, found: 288.0881.

4.2.5. 2′-*O*-Carbamoyl-5′-*O*-(4,4′-dimethoxytrityl)uridine 3′-(2-cyanoethyl *N*,*N*-diisopropylphosphoramidite) 5

Compound **3** (1.3 g, 2.2 mmol) was rendered anhydrous by repeated co-evaporation thrice each with anhydrous pyridine, anhydrous toluene, and anhydrous CH_2Cl_2, and the residue was finally dissolved in anhydrous CH_2Cl_2 (22 mL). To this solution were added diisopropylamine (155 μL, 1.1 mmol), 1*H*-tetrazole (77 mg, 1.1 mmol), and bis(*N*,*N*-diisopropylamino)phosphine (839 μL, 2.6 mmol). After the resulting mixture was stirred for 2 h, the reaction was quenched by adding water (1 mL), and the mixture was diluted with ethyl acetate (50 mL). The organic layer was washed five times with 5% Na_2CO_3, dried over Na_2SO_4, filtered, and concentrated to dryness. The residue was chromatographed on a silica gel column (26 g) with chloroform–methanol (100:2–100:4, v/v) containing 0.5% triethylamine to give **5** (0.89 g, 51%). ^{1}H NMR ($CDCl_3$) δ 1.06–1.27 (14H, m), 2.42 (1H, m, CH_2 of cyanoethyl), 2.69 (1H, m), 3.42–3.53 (2H, m), 3.57–3.70 (2H, m), 3.79 (6H, d, J = 2.9 Hz), 4.12 (1H, m), 4.21–4.31 (1H, m), 4.67 (1H, m), 4.69 (2H, d, J = 3.2 Hz), 5.30–5.43 (2H, m), 6.22 (1H, m), 6.84 (4H, m), 7.24–7.40 (9H, m), 7.70 (1H m), 8.11 (1H, m); ^{13}C NMR ($CDCl_3$) δ 14.5, 20.4, 24.8, 43.5, 55.5, 58.2, 60.6, 63.1, 71.3, 75.5, 84.5, 86.2, 87.5, 103.1, 113.6, 127.5, 128.5, 130.5, 135.2, 140.3, 144.3, 150.7, 155.5, 159.0, 162.8; ^{31}P NMR ($CDCl_3$) δ 151.2, 151.5. MS *m/z* calculated for $C_{40}H_{49}N_5O_{10}P^+$ $[M+H]^+$: 790.2312, found: 790.3297.

4.3. Synthesis of oligonucleotides incorporating 2′-*O*-carbamoyluridine

Oligodeoxynucleotides and 2′-*O*-Me-oligoribonucleotides incorporating 2′-*O*-carbamoyluridine, 5′-d(GTACC)[U_{cm}]d(TTCCGG)-3′, and 5′-$G_{OMe}U_{OMe}A_{OMe}C_{OMe}C_{OMe}$[$U_{cm}$]$U_{OMe}U_{OMe}C_{OMe}C_{OMe}G_{OMe}G_{OMe}$-3′, respectively, were synthesized as follows. First, 3′-half sequences, 5′-d(TTCCGG)-3′, and $U_{OMe}U_{OMe}C_{OMe}C_{OMe}G_{OMe}G_{OMe}$, were synthesized using an Applied Biosystems 394 automated DNA/RNA synthesizer by the standard 1.0-μmol-scale phosphoramidite approach for DNA and RNA, respectively, which consists of detritylation, coupling, capping, and iodine oxidation steps. The CPG support was removed from a cartridge column and placed on a glass syringe having a glass filter. Then, a U_{cm} unit was introduced into the 5′-terminal position by use of 20 equiv of the phosphoramidite derivative **5** and 80 equiv of 1*H*-tetrazole by use of 250 μL of dry CH_3CN. The coupling time was 5 min. After this manual procedure, the CPG support was placed back in the cartridge column, and the remaining 5′-half sequences, 5′-d(GTACC)-3′ and 5′-$G_{OMe}U_{OMe}A_{OMe}C_{OMe}C_{OMe}$-3′, were synthesized in the automated synthesizer. Release of the resulting protected 5′-*O*-DMTr-oligonucleotide from the solid support and deprotection of the phosphate and base-protecting groups were performed by treatment with 28% aqueous ammonia at room temperature for 24 h. The solution was evaporated under reduced pressure at room temperature to remove ammonia, and the residue was diluted with 0.1 M ammonium acetate (50 mL). The solution was placed on a C18 cartridge column, and the failure sequences were eluted using 10% CH_3CN/0.1 M ammonium acetate as an eluent. After washing with 0.1 M ammonium acetate and water, the column was treated with aqueous 2% TFA to remove the DMTr group and further washed with 0.1 M ammonium acetate and water. The target oligonucleotide was eluted using 20% CH_3CN/water, and the fractions containing the target were lyophilized to give the crude oligonucleotide. Pure material was obtained by anion-exchange HPLC using a 0–50% gradient of 1 M NaCl in 25 mM sodium phosphate–10% CH_3CN. The salts were removed using a C18 cartridge column to give the pure oligonucleotide after being lyophilized to dryness. The yields of the pure materials were 26% for the DNA and 33% for the 2′-*O*-Me-RNA. These yields were calculated assuming that the molar extinction coefficients of 5′-GTACC[U_{cm}]TTCCGG-3′ and 5′-$G_{OMe}U_{OMe}A_{OMe}C_{OMe}$-$C_{OMe}$[$U_{cm}$]$U_{OMe}U_{OMe}C_{OMe}C_{OMe}G_{OMe}G_{OMe}$-3′ were identical to those of 5′-GTACCTTTCCGG-3′ and 5′-GUACCUUUCCGG-3′, respectively. The structures were confirmed by MALDI-TOF mass spectroscopy. MALDI-TOF mass of 5′-GTACC[U_{cm}]TTCCGG-3′ $[M + H]^+$: calculated 3657.5, found: 3656.6; MALDI-TOF mass of 5′-$G_{OMe}U_{OMe}A_{OMe}C_{OMe}$-$C_{OMe}$[$U_{cm}$]$U_{OMe}U_{OMe}C_{OMe}C_{OMe}G_{OMe}G_{OMe}$-3′ $[M+H]^+$: calculated 3946.1, found: 3947.1.

4.4. CD spectra

CD spectra were measured using 2 μM solutions of the duplexes in 10 mM sodium phosphate (pH 7.0) containing 150 mM NaCl and 0.1 mM EDTA at 10 °C.

4.5. T_m measurement

Each oligonucleotide was dissolved in 10 mM sodium phosphate (pH 7.0) containing 150 mM NaCl and 0.1 mM EDTA so that the final concentration of each oligonucleotide became 2 μM. The solution was separated into quartz cells (10 mm) and incubated at 85 °C. After 10 min, the solution was cooled to 5 °C at a rate of 0.5 °C/min and heated to 85 °C at the same rate. During this annealing and melting, the absorption at 260 nm was recorded and used to draw UV-melting curves. The T_m value was calculated as the temperature that gave the maximum of the first derivative of the UV-melting curve.

4.6. MD simulation

The atomic charges of 2′-*O*-carbamoyluridine were estimated from the ab initio calculation at the HF/6-31G* level performed using Gaussian03.[38] The structures obtained by two 5.4-ns MD simulations of the 2′-*O*-Me RNA and RNA duplex containing the 2′-*O*-$CONH_2$ group at the central position, at constant temperature (300 K) and pressure (1 atm), were generated using the AMBER 9.0 molecular simulation package.[39]

(i) System setup
The duplexes were placed in a box containing 32 Na^+ and 10 Cl^- in addition to 3631 TIP3P water molecules corresponding to a concentration close to 0.15 M NaCl. The initial structures were generated using the NUCGEN module of AMBER. In this calculation, the all-atom force field described by Cornell et al. was employed.[34] The box dimensions were chosen such that they ensured a 10-Å solvation shell around the duplexes.

(ii) MD simulation
The equilibration procedure consisted of 200 steps of steepest descent minimization without positional constraints, followed by eight 50-ps MD simulations in which the solute atoms were fixed at the initial positions. Then, the next seven 50-ps MD runs were performed with positional constraints on the nucleic acid atoms of 10, 5, 2, 1, 0.5, 0.1, and 0.01 kcal/mol. After the 400-ps equilibration phase, a 5.0-ns production run was performed from which only the data of the last 200 ps were used to calculate the average structure.

Acknowledgments

This study was supported by Industrial Technology Research Grant Program in ′05 from the New Energy and Industrial Technology Development Organization (NEDO) of Japan. This study was also supported by a Grant-in-Aid for Scientific Research (B) 20350074.

References and notes

1. Czauderna, F.; Fechtner, M.; Dames, S.; Aygun, H.; Klippel, A.; Pronk, G. J.; Giese, K.; Kaufmann, J. *Nucleic Acid Res.* **2003**, *31*, 2705.
2. Chiu, Y.; Rana, T. M. *RNA* **2003**, *9*, 1034.
3. Jackson, A.; Burchard, J.; Leake, D.; Reynold, A.; Schelter, J.; Guo, J.; Johnson, J. M.; Lim, L.; Karpilow, J.; Nichols, K.; Marshall, W.; Khvorova, A.; Linsley, P. S. *RNA* **2006**, *12*, 1197.
4. Bryan, A.; Kraynack, B. A.; Baker, A. F. *RNA* **2006**, *12*, 163.
5. Beuvink, I.; Kolb, F. A.; Budach, W.; Granier, A.; Lange, J.; Natt, F.; Dengler, U.; Hall, J.; Filipowicz, W.; Weiler, J. *Nucleic Acids Res.* **2007**, *35*, e52.
6. Freier, S. M.; Altmann, K.-H. *Nucleic Acids Res.* **1997**, *25*, 4429.
7. Inoue, H.; Hayase, Y.; Imura, A.; Iwai, S.; Miura, K.; Ohtsuka, E. *Nucleic Acids Res.* **1987**, *15*, 6131.
8. Martin, P. *Helv. Chim. Acta* **1995**, *78*, 486.
9. Martin, P. *Helv. Chim. Acta* **1996**, *79*, 1930.
10. Martin, P. *Helv. Chim. Acta* **2003**, *86*, 204.
11. Baker, B. F.; Lot, S. S.; Condon, T. P.; Cheng-Flournoy, S.; Lesnik, E. A.; Sasmor, H. M.; Bennett, C. F. *J. Biol. Chem.* **1997**, *272*, 11994.
12. Teplova, M.; Minasov, G.; Tereshko, V.; Inamati, G. B.; Cook, P. D.; Manoharan, M.; Egli, M. *Nat. Strut. Biol.* **1997**, *6*, 535.
13. Maier, M. A.; Guzaev, A. P.; Manoharan, M. *Org. Lett.* **2000**, *2*, 1819–1822.
14. Rajeev, K. G.; Prakash, T. P.; Manoharan, M. *Org. Lett.* **2003**, *5*, 3005.
15. Yu, R. Z.; Geary, R. S.; Monteith, D. K.; Matson, J.; Truong, L.; Fitchett, J.; Levin, A. A. *J. Pharm. Sci.* **2004**, *93*, 48.
16. Grotli, M.; Douglas, M.; Eritja, R.; Sproat, B. S. *Tetrahedron* **1998**, *54*, 5899.
17. Griffey, R. H.; Monia, B. P.; Cummins, L. L.; Freier, S.; Greig, M. J.; Guinosso, C. J.; Lesnik, E.; Manalili, S. M.; Mohan, V.; Owens, S.; Ross, B. R.; Sasmor, H.; Wancewicz, E.; Weiler, K.; Wheeler, P. D.; Cook, P. D. *J. Med. Chem.* **1995**, *39*, 5100–5109.
18. Prakash, T. P.; Manoharan, M.; Fraser, A. S.; Kawasaki, A. M.; Lesnik, E. A.; Owens, S. R. *Tetrahedron Lett.* **2000**, *41*, 4855.
19. Prakash, T. P.; Kawasaki, A. M.; Lesnik, E. A.; Owens, S. R.; Manoharan, M. *Org. Lett.* **2003**, *5*, 403.
20. Pattanayek, R.; Sethaphong, L.; Pan, C.; Prhavc, M.; Prakash, T. P.; Manoharan, M.; Egli, M. *J. Am. Chem. Soc.* **2004**, *126*, 15006.
21. Saneyoshi, H.; Seio, K.; Sekine, M. *J. Org. Chem.* **2005**, *70*, 10453.
22. Sundaralingam, M.; Pan, B. *Biophys. Chem.* **2002**, *95*, 273.
23. Auffinger, P.; Westhof, E. *Angew. Chem., Int. Ed.* **2001**, *40*, 4648.
24. Auffinger, P.; Westhof, E. *J. Mol. Biol.* **2000**, *300*, 1113.
25. Banerjee, R.; Maji, S. K.; Banerjee, A. *Acta Crystallogr., Sect. C* **2000**, *56*, 1120.
26. Semetey, V.; Hemmerlin, C.; Didierjean, C.; Schaffner, A. P.; Giner, A. G.; Aubry, A.; Briand, J. P.; Marraud, M.; Guichard, G. *Org. Lett.* **2001**, *3*, 3843–3846.
27. Miyata, K.; Kobori, A.; Tamamushi, R.; Ohkubo, A.; Taguchi, H.; Seio, K.; Sekine, M. *Eur. J. Org. Chem.* **2006**, 3626–3637.
28. Markiewicz, W. T.; Biala, E.; Kierzek, R. *Bull. Pol. Acad. Sci., Chem.* **1984**, *32*, 433.
29. Westman, E.; Stromberg, R. *Nucleic Acids Res.* **1994**, *22*, 2430.
30. Hayakawa, Y.; Kataoka, M. *J. Am. Chem. Soc.* **1998**, *120*, 12395.
31. Altona, C. *Recl. Trav. Chim. Pays-Bas* **1982**, *101*, 413.
32. Prhavc, M.; Lesnik, E. A.; Mohan, V.; Manoharan, M. *Tetrahedron Lett.* **2001**, *42*, 8777.
33. Lesnik, E. A.; Guinosso, C. J.; Kawasaki, A. M.; Sasmor, H.; Zounes, M.; Cummins, L. L.; Ecker, D. J.; Cook, P. D.; Freier, S. M. *Biochemistry* **1993**, *32*, 7832.
34. Cornell, W. D.; Cieplak, P.; Bayly, C. I.; Gould, I. R.; Merz, K. M., Jr.; Ferguson, D. M.; Spellmeyer, D. C.; Fox, T.; Caldwell, J. W.; Kollman, P. A. *J. Am. Chem. Soc.* **1995**, *117*, 5179.
35. Biswas, R.; Sundaralingam, M. *J. Mol. Biol.* **1997**, *270*, 511.
36. Biswas, R.; Wahl, M. C.; Ban, C.; Sundaralingam, M. *J. Mol. Biol.* **1997**, *267*, 1149.
37. Shi, K.; Wahl, M.; Sundaralingam, M. *Nucleic Acids Res.* **1999**, *27*, 2196.
38. Frisch, M. J.; Trucks, G. W.; Schlegel, H. B.; Scuseria, G. E.; Robb, M. A.; Cheeseman, J. R.; Montgomery, J. A.; Jr.; Vreven, T.; Kudin, K. N.; Burant, J. C.; Millam, J. M.; Iyengar, S. S.; Tomasi, J.; Barone, V.; Mennucci, B.; Cossi, M.; Scalmani, G.; Rega, N.; Petersson, G. A.; Nakatsuji, H.; Hada, M.; Ehara, M.; Toyota, K.; Fukuda, R.; Hasegawa, J.; Ishida, M.; Nakajima, T.; Honda, Y.; Kitao, O.; Nakai, H.; Klene, M.; Li, X.; Knox, J. E.; Hratchian, H. P.; Cross, J. B.; Bakken, V.; Adamo, C.; Jaramillo, J.; Gomperts, R.; Stratmann, R. E.; Yazyev, O.; Austin, A. J.; Cammi, R.; Pomelli, C.; Ochterski, J. W.; Ayala, P. Y.; Morokuma, K.; Voth, G. A.; Salvador, P.; Dannenberg, J. J.; Zakrzewski, V. G.; Dapprich, S.; Daniels, A. D.; Strain, M. C.; Farkas, O.; Malick, D. K.; Rabuck, A. D.; Raghavachari, K.; Foresman, J. B.; Ortiz, J. V.; Cui, Q.; Baboul, A. G.; Clifford, S.; Cioslowski, J.; Stefanov, B. B.; Liu, G.; Liashenko, A.; Piskorz, P.; Komaromi, I.; Martin, R. L.; Fox, D. J.; Keith, T.; Al-Laham, M. A.; Peng, C. Y.; Nanayakkara, A.; Challacombe, M.; Gill, P. M. W.; Johnson, B.; Chen, W.; Wong, M. W.; Gonzalez, C.; Pople, J. A. Gaussian 03, Revision C.02, 2004.
39. Case, A.; Darden, T. A.; Cheatham, T. E., III, Simmerling, C. L.; Wang, J.; Duke, R. E.; Luo, R.; Merz, K. M.; Pearlman, D. A.; Crowley, M.; Walker, R. C.; Zhang, W.; Wang, B.; Hayik, S.; Roitberg, A.; Seabra, G.; Wong, K. F.; Paesani, F.; Wu, X.; Brozell, S.; Tsui, V.; Gohlke, H.; Yang, L.; Tan, C.; Mongan, J.; Hornak, V.; Cui, G.; Beroza, P.; Mathews, D. H.; Schafmeister, C.; Ross, W. S. and Kollman, P. A. AMBER 9.0.